Update in
Anaesthesia

Basic principles of ultrasound and the use of lung ultrasound in the COVID-19 pandemic

Edmund Chan*, Dr Nishita Desai, Dr Francesca Elwen, Dr Michael Trauer, Dr Heather Mulrenan and Dr Neel Desai
*Correspondence email: edmund.chan@doctors.org.uk
doi: 10.1029/WFSA-D-20-00019

Abstract

Given that ultrasound use is increasing in healthcare, operators must be familiar with its physics in order to optimise the image and interpret potential artifacts. Ultrasound are sound waves at frequencies above the range of human hearing, that are transmitted from and received by an ultrasound transducer with piezoelectric properties. As it propagates through tissues, some of the ultrasound waves are reflected at tissue boundaries, leading to its detection by the ultrasound transducer. These are processed by the ultrasound machine and result in the generation of an image.

Various settings can be adjusted to optimise the image, such as the frequency of the transmitted ultrasound wave, depth of the focal zone and the gain. Artifacts are presentations on the monitor of the ultrasound machine which are added, omitted, or are of improper brightness, location, shape, and size compared with true anatomical features. It can result in falsely perceived objects, missing structures or degraded images. The presence or absence of such artifacts in lung ultrasound can be valuable in the interpretation of the resulting image. In the setting of COVID-19, lung ultrasound has become increasingly useful in evaluating disease progression and providing a point-of-care radiological adjunct in clinical decision making.

Key words: acoustic artifacts; acoustic impedance; coronavirus disease; lung ultrasound; pneumonia; severe acute respiratory syndrome; COVID-19; spatial resolution; temporal resolution; ultrasonic waves; ultrasonography

INTRODUCTION

Ultrasound is defined as sound waves characterised by frequencies above the range of human hearing, that is greater than twenty kilohertz[1]. Its use in imaging has become increasingly commonplace in healthcare, with a broad array of diagnostic and therapeutic applications across a wide range of medical specialities in both resource-rich and resource-poor countries[2]. In view of the growing availability, portability and the technological advancement of ultrasound, its utility continues to evolve with increasing applications at the point of patient care beyond traditional radiological as well as obstetric and gynaecological indications. Examples of this include the focused scanning of particular body systems to serve as an adjunct to clinical assessment[3]. In particular, lung ultrasound (LUS) has been suggested to be a valuable imaging modality in the current COVID-19 pandemic, precipitated by the SARS-CoV-2 virus[4]. The use of ultrasound has also been recommended by the various Royal College or Society guidelines in order to facilitate procedures such as the placement of central venous catheters or chest drains[5,6]. Further, ultrasound is extensively used in the targeted injection of local anaesthetic around nerves in regional anaesthesia[7].

Our review aims to discuss the basic principles of ultrasound, fundamentals of image generation and optimisation, artifacts that can be produced, and the role of LUS in the current COVID-19 pandemic.

Characteristics of ultrasound

Sound can be defined as longitudinal pressure waves, with alternating compression and rarefaction, that are propagated through a medium. It is characterised by amplitude, frequency, wavelength, and speed (Figure 1). Amplitude, measured in decibels (dB), is the maximum displacement of a point in the wave from equilibrium. The frequency (f) of an ultrasound wave is the number of cycles, or pressure peaks, occurring in one second and is measured in hertz (Hz). Medical ultrasound has a frequency of between one to twenty megahertz (MHz). Its wavelength (λ), inversely proportional to the frequency, is the distance between

Dr Edmund Chan
MA BMBCH FRCA MACADMED
Fellow in Paediatric Anaesthesia
Great Ormond Street Hospital for Children NHS Foundation Trust
London
UNITED KINGDOM

Dr Nishita Desai BSC (HONS) MB BS FFICM MRCP MSC
Consultant in Intensive Care Medicine
Guy's and St Thomas' Hospitals NHS Foundation Trust
London
UNITED KINGDOM

Dr Francesca Elwen MB CHB BSC
Specialty Registrar in Anaesthesia
Ashford and St Peter's Hospitals NHS Foundation Trust
Chertsey
UNITED KINGDOM

Dr Michael Trauer MBBS (MONASH) FRCEM PGD (MEDICAL ULTRASOUND)
Consultant in Emergency Medicine
Guy's and St Thomas' Hospitals NHS Foundation Trust
London
UNITED KINGDOM

Dr Heather Mulrenan MBBS MSC
Lewisham and Greenwich NHS Trust
London
UNITED KINGDOM

Dr Neel Desai MB CHB (HONS) BSC (HONS) FHEA FRCA EDRA MRCP MRCS PGCERT MEDICAL EDUCATION DIP REG ANAESTH
Consultant Anaesthetist
Guy's and St Thomas' Hospitals NHS Foundation Trust
London
UNITED KINGDOM

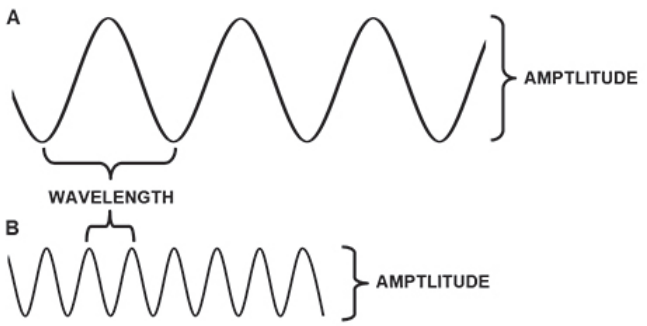

Figure 1: Characteristics of an ultrasound wave with lower frequency, longer wavelength and larger amplitude (A) and higher frequency, shorter wavelength and lower amplitude (B)

the pressure peaks and is measured in metres[1]. The speed (c) of ultrasound is dependent on the physical properties of the medium through which it is propagated and is measured in metres per second (ms-1). Speed, frequency, and wavelength are related to each other in the equation:

$$c = f \times \lambda$$

Ultrasound has a speed of 330, 1450 and 1540 m s-1, respectively, in air, fatty tissue and soft tissue.

Generation of an ultrasound image

In order to generate an image with ultrasound, sound waves are transmitted from and received by an ultrasound transducer, the latter containing ferroelectric polycrystalline ceramic materials with piezoelectric properties such as lead zirconate titanate[8]. In the reverse piezoelectric effect, under the influence of an alternating current, the crystalline material of the transducer expands and contracts as the polarity of the voltage changes, and the consequent vibrations produce the pulse of an ultrasound wave of two or three cycles of the desired frequency.

Once the ultrasound pulse has been generated, the transducer changes from emitting to receiving mode. Due to its interaction with the interfaces present within the medium, a variable proportion is reflected back to the ultrasound transducer. This reflected ultrasound wave results in the secondary mechanical deformation of the crystalline material of the transducer through the piezoelectric effect and is transformed into electrical current. In this manner, the ultrasound transducer functions as a speaker and a microphone where the process of transmission and reception is repeated thousands of times per second[1].

In the generation of the image on the monitor of the ultrasound machine, the amplitude of the reflected ultrasound wave determines the brightness of an echo pixel on a grey scale. Structures that strongly reflect the ultrasound wave are brighter or hyperechoic and those that weakly reflect it are darker or hypoechoic. The horizontal position of the echo pixel on the screen is dependent on the position of the receiving piezoelectric crystalline material on the ultrasound transducer. The vertical position, or depth, of the echo pixel reflects the time delay between the emission and the receipt of the ultrasound wave. It is this pattern of the brightness and the position of the echo pixels that results in the fundamental B-mode image[9].

Ultrasound interaction with tissues

As the ultrasound wave propagates through the body, it interacts with tissues and, in doing so, is reflected, refracted, and attenuated (Figure 2).

Reflection

If an ultrasound wave encounters an interface between two tissues of different acoustic impedance, part of the sound energy is reflected, and the remainder is transmitted. The acoustic impedance of a tissue (Z), measured in Rayls, is defined as a product of its density (ρ) and the speed of ultrasound (c) through that particular tissue, and is a measure of the tissue's tendency to resist the passage of an ultrasound wave:

$$Z = \rho \times c$$

Compared to soft tissue, air has a lower acoustic impedance and bone has a higher acoustic impedance. Should the mismatch between the acoustic impedances of two tissues that form an interface be greater, then more of the sound energy is reflected rather than transmitted.

The nature of the reflection of the ultrasound wave can be either specular or scattered. In specular reflection, the interface is large and smooth, its dimensions larger than the wavelength of the ultrasound wave, and the reflector is like a mirror. Its reflectivity to the ultrasound transducer is most when the angle of incidence of the ultrasound wave is perpendicular to the reflector (Figure 3). In scattering, the dimensions of the reflector are smaller than the wavelength of the ultrasound wave or the interface is rough and irregular, and the ultrasound wave is reflected through a wide range of angles. Given this, less of the reflected ultrasound wave is directed towards the ultrasound transducer, but several organs such as the liver have characteristic scatter signatures that reflect their underlying structures[10].

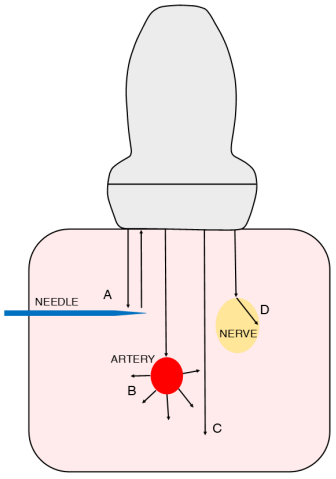

Figure 2: Once the ultrasound wave has been emitted from the ultrasound transducer, it can interact at interfaces with tissues to undergo specular reflection (A), scatter reflection (B), transmission (C) and refraction (D)

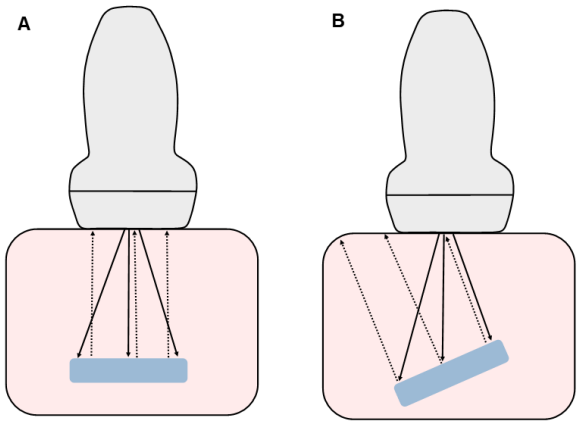

Figure 3: If the reflector is perpendicular to the ultrasound wave, then most of the ultrasound wave is reflected to the ultrasound transducer (A) and the reflector is well imaged. Should this not be the case with a decreased angle of insonation, then much of the ultrasound wave is reflected away from the ultrasound transducer (B) and the view of the target is not optimal

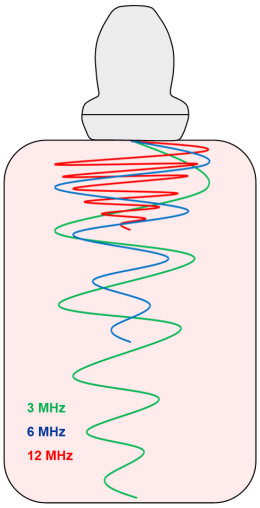

Figure 4: In the presence of higher frequency ultrasound waves and longer ultrasound path lengths, attenuation or energy loss is increased

Refraction

Once an ultrasound wave has reached an interface between two tissues of different acoustic velocities, the part of the sound energy that is transmitted is likely to change its direction of travel or refract, unless its angle of incidence is perpendicular. It does this because the wavelength rather than the frequency of the ultrasound wave is modified to accommodate the differences, however small, in the speed of ultrasound through those tissues.

Attenuation

Attenuation refers to the progressive loss of sound energy as the ultrasound wave passes through tissue. It is related mainly to the conversion of some of the energy into heat by induced oscillatory motion of the tissues in a process known as absorption, and is increased in the presence of higher frequency ultrasound waves and longer ultrasound path lengths (Figure 4). Further, different tissues have varying attenuation coefficients and the higher the attenuation coefficient, the more attenuated the ultrasound waves are by the specified tissue[9]. Compared to soft tissue, blood has a lower attenuation coefficient, and air and bone have higher attenuation coefficients.

Spatial resolution

Spatial resolution can be defined as the ability of the ultrasound machine to determine two points as separate entities in space and is subcategorised into axial and lateral resolution.

Axial resolution

Axial resolution is the minimum distance that can be differentiated between two reflectors located parallel to the direction of the ultrasound beam[7]. It is mathematically equal to half the spatial pulse length, that is the product of the number of cycles of the pulse of an ultrasound wave and its wavelength (Figure 5).

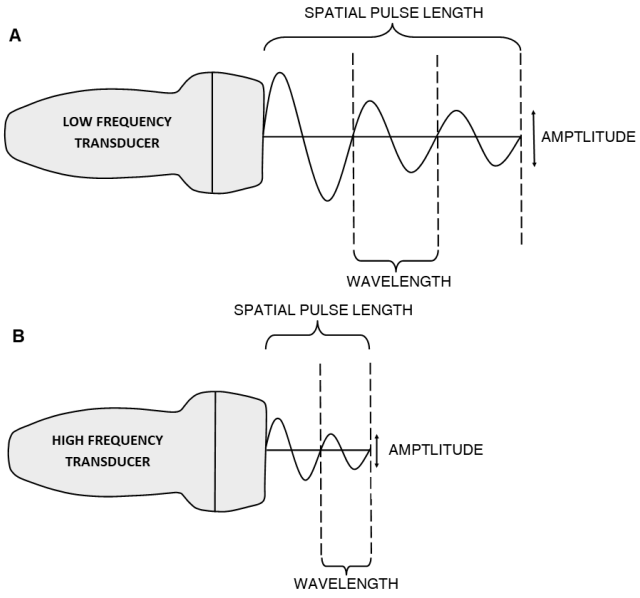

Figure 5: Illustration of a low frequency ultrasound transducer with long spatial pulse length and a consequent low axial resolution (A) and a high frequency transducer with short spatial pulse length and a corresponding high axial resolution (B)

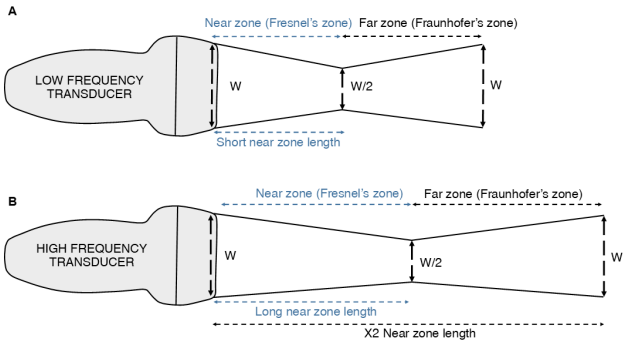

Figure 6: Illustration of a low frequency ultrasound transducer with a short near zone length (A) and a high frequency ultrasound transducer with a long near zone length (B). W: width

If the spatial pulse length is short, as it would be with an ultrasound wave of high frequency and hence short wavelength, then the axial resolution is high[11].

Lateral resolution

Lateral resolution is the minimum distance that can be differentiated between two reflectors located perpendicular to the direction of the ultrasound beam. At the level of the ultrasound transducer, the width of the ultrasound beam is equal to that of the ultrasound transducer (Figure 6).

The ultrasound beam then converges to its narrowest width, that is half of the width of the ultrasound transducer, at the near zone length. As the ultrasound wave passes beyond the near zone into the far zone, the ultrasound beam diverges till its width is once again equal to that of the ultrasound transducer at twice the near zone length.

If the near zone length is long, as it would be with an ultrasound wave of high frequency and thus short wavelength, then the lateral resolution is high with shorter distances between adjacent element ultrasound beams[11]. Lateral resolution is highest in the focal zone where the ultrasound beam is at its narrowest. Should the ultrasound beam be divergent, then the reflector can be overlooked by slipping in between these element ultrasound beams.

Doppler ultrasound

In the Doppler effect, the emission or reflection of a wave by a moving object will change its frequency as the object moves away or towards a stationary listener, the latter in this case an ultrasound transducer. If an object moves towards the ultrasound transducer, the wavelength of the sound waves travelling towards it are compressed, leading to a higher frequency. Should an object move away from the ultrasound transducer, the wavelength of the sound waves travelling away from it are stretched, resulting in a lower frequency.

It is this change in frequency of the reflected ultrasound wave that can be detected by the ultrasound transducer in order to calculate the velocity of a moving reflector (v) with the Doppler shift equation[10]:

$$v = \frac{f_d c}{2 f_0 \cos\theta}$$

where θ is the Doppler angle, in other words the angle of insonation between the direction of travel of the measured object and the direction of the ultrasound wave; c is the speed of sound in the medium; f_d is the Doppler frequency shift, that is the difference between the emitted and the detected frequencies; and f_0 is the emitted frequency.

Blood flow can be measured indirectly with the Doppler shift equation and information related to such moving reflectors can be superimposed onto a B-mode image with colour Doppler.

Practical implications

Choosing the most appropriate frequency of the transmitted ultrasound wave is a compromise between the axial resolution and the depth of penetration. Higher frequencies of ultrasound wave provide superior axial resolution of superficial structures but have increased attenuation and consequent decreased tissue penetration. Lower frequencies of ultrasound wave result in deeper tissue penetration at the expense of axial resolution.

In order to limit the effect of attenuation on the quality of the image on the monitor, the gain dial on the ultrasound machine can be adjusted. Gain is defined as the amplification of the intensity of the returning ultrasound wave, and hence the brightness of the echoes, across all points in the displayed field.

Given that attenuation is increased in the presence of longer ultrasound path lengths, time gain compensation facilitates the independent manipulation of the image brightness as a function of time and thus at specific depths in the field. It can be set up to selectively amplify the more attenuated ultrasound waves returning from deeper structures without overamplification of the ultrasound waves from more superficial tissues.

The focus or focal zone, indicated on the monitor of the ultrasound machine and representing the narrowest part of the ultrasound beam, can be positioned at the depth of the area of interest to increase lateral resolution. Several focal zones can be implemented to maintain lateral resolution with increased depth, but at the expense of temporal resolution as the ultrasound transducer must emit and process the ultrasound wave directed at each focal length[12].

If a target structure is of a different acoustic impedance to the surrounding tissue, then a greater proportion of the ultrasound wave is reflected at this interface and the target structure can be differentiated more easily. The position and direction of the ultrasound beam is important. In Doppler ultrasound, blood flow is best imaged if the ultrasound beam is aligned in its direction. Blood flow is not visualised should the blood vessels be perpendicular to the ultrasound beam[13].

Artifacts

Artifacts are presentations on the monitor of the ultrasound machine that are added or omitted or are of improper brightness, location, shape, and size compared with the true anatomical features. In some contexts, artifacts can be beneficial. LUS, in particular, relies on the interpretation of artifacts generated in the context of a predominantly aerated lung[14]. In other scenarios, artifacts can cause confusion and error.

Acoustic artifacts

Acoustic artifacts are normally due to incorrect assumptions occurring in the processing by the instrumentation. It can result in either falsely perceived objects and missing structures, or degraded images. Examples of the former include overgain and undergain artifacts, acoustic enhancement and shadowing. Examples of the latter are secondary to reverberation, ensuing as a result of the ultrasound wave reflecting repeatedly between two specular reflectors.

Dropout shadows occur with loss of contact between the faceplate of the ultrasound transducer and the skin of the patient. It can be corrected with adequate conductive gel and optimal contact and positioning of the ultrasound transducer[13]. In overgain and

undergain artifacts, too high and low a gain, respectively, can obscure a structure or make a structure appear absent (Figure 7). In acoustic enhancement, a structure such as a blood vessel with a low attenuation coefficient weakly attenuates the ultrasound wave and the region immediately deep to it produces stronger echoes, falsely enhancing compared to surrounding structures (Figure 8). In acoustic shadowing, a structure, such as bone, with a high acoustic impedance and attenuation coefficient strongly absorbs or reflects the ultrasound wave and the region immediately deep to it produces weaker echoes. In the context of LUS, this is of particular relevance given the presence of aerated lung and ribs. Reverberation artifacts can occur in various settings. Needle visualisation for the insertion of vascular access catheters or regional anaesthesia may lead to needle reverberation artifact, where portions of the ultrasound wave undergo a varying number of reflections within the lumen of the needle. This results in the staggered return of the trapped ultrasound wave to the ultrasound transducer and the occurrence of multiple linear and hyperechoic lines deep and parallel to the reflecting surface (Figure 9)[13]. In the context of LUS, A-lines represent reverberation artifacts as well[14], and are discussed in more detail below.

Anatomic artifacts

Anatomic artifacts are tissues which resemble the target structures, such as blood vessels, lymph nodes, nerve and tendons[13].

Lung ultrasound and COVID-19

LUS has demonstrated itself to be a valuable point-of-care diagnostic modality in the assessment, monitoring and the management of patients with pulmonary manifestations due to COVID-19[4,15,16]. It has the capacity to identify parenchymal and pleural disease with high sensitivities[17], even if pulmonary pathology owing to COVID-19 does not have specific pathognomonic findings on ultrasound[18].

How to perform lung ultrasound

LUS is best performed through the intercostal space as the acoustic window. Given the high acoustic impedance and attenuation coefficient of air compared to soft tissue such as the pleura, the ratio of air and fluid in the lung underlying the pleura determines whether the image on the monitor of the ultrasound machine characterises only artifacts, as is the case in normal aerated lung, or is a direct depiction of tissue, as is the case in abnormally fluid-filled lung.

If available, the microconvex probe that has an ultrasound frequency of 3–5 MHz is optimal for LUS. Other ultrasound probes, however, are more widely available, and these include the linear, curvilinear and phased array ones. The linear ultrasound transducer enables a better definition of the subpleural space yet is limited by a narrow sector width and poor tissue penetration due to its high frequency, and the phased array probe has a smaller footprint that gives rise

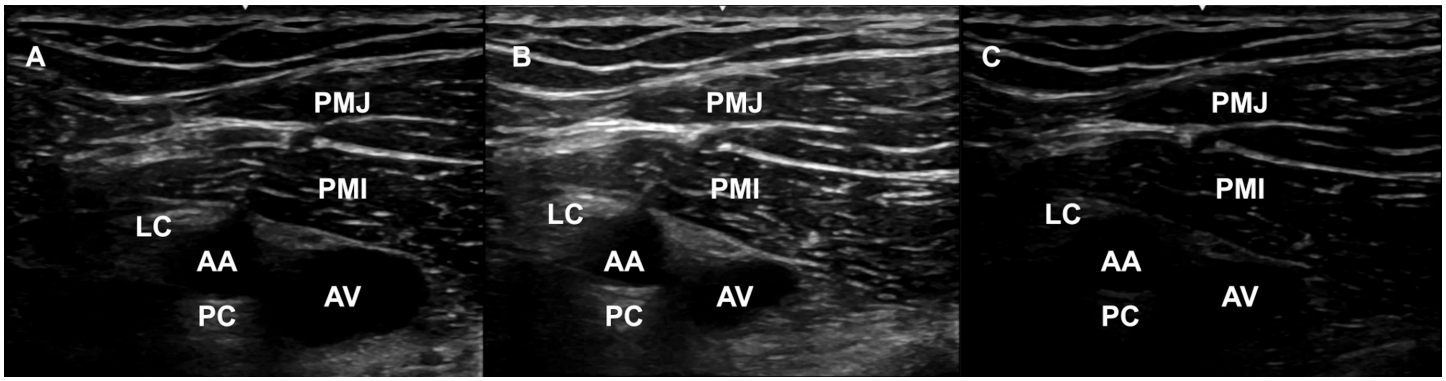

Figure 7: Ultrasound image of the infraclavicular fossa with the correct gain setting (A) compared to too high (B) or too low (C) gain. AA: axillary artery; AV: axillary vein; LC: lateral cord of brachial plexus; PC: posterior cord of brachial plexus; PMI: pectoralis minor muscle; PMJ: pectoralis major muscle

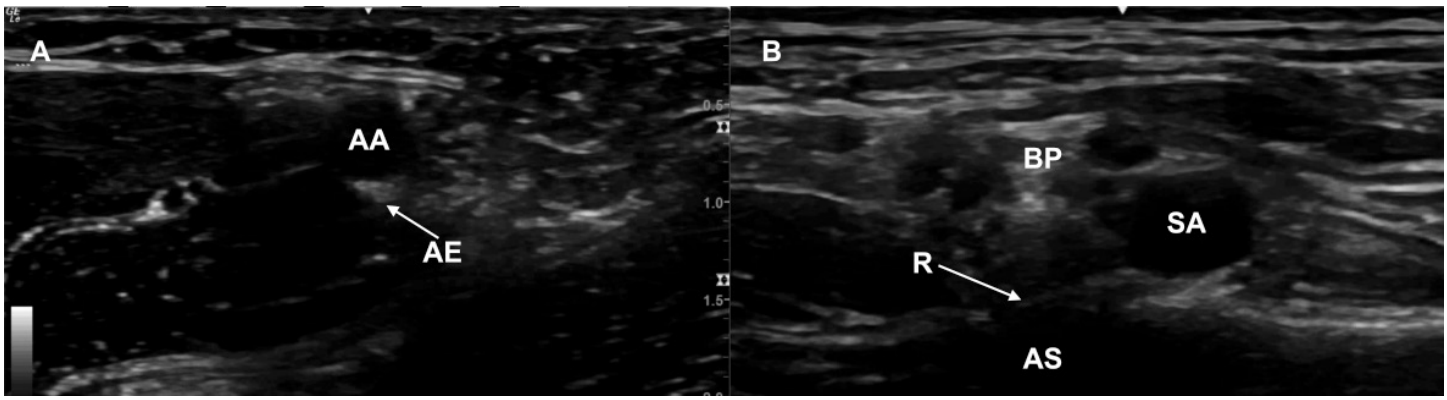

Figure 8: Ultrasound image of the axillary fossa demonstrating acoustic enhancement of the structure immediately deep to the axillary artery (A) and of the supraclavicular fossa showing acoustic shadowing deep to the first rib (B). AA: axillary artery; AE: acoustic enhancement; AS: acoustic shadowing; BP: brachial plexus; R: rib; SA: subclavian artery

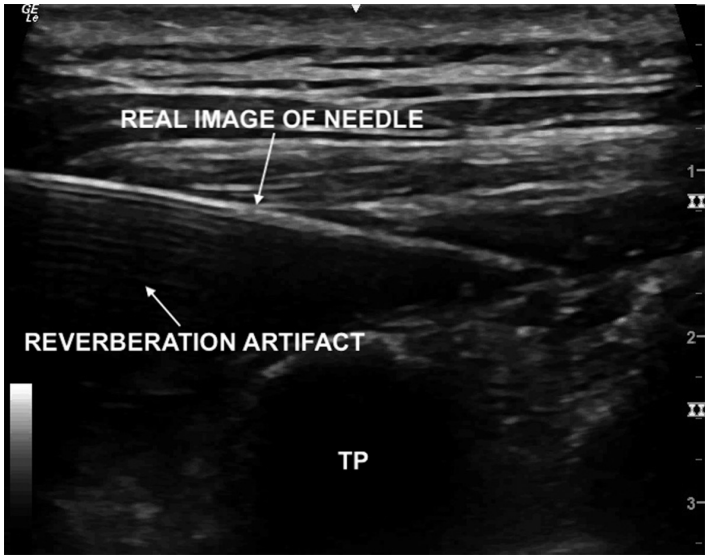

Figure 9: Ultrasound image of the transverse processes and overlying musculature. The needle can be visualised in long axis with underlying needle reverberation artifact. TP: transverse process

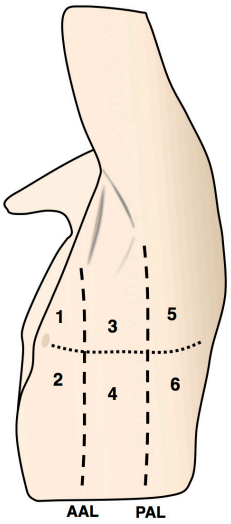

Figure 10: Ultrasound image of the transverse processes and overlying musculature. The needle can be visualised in long axis with underlying needle reverberation artifact. TP: transverse process

to improved access to the intercostal space, albeit with poorer image resolution. The curvilinear probe has a significant footprint and therefore can decrease dexterity across the narrow intercostal windows. Fundamentally, the choice of ultrasound probe is dependent on local availability as well as operator experience and preference. Importantly, many modern ultrasound machines have a built in lung preset that will deactivate compound and harmonic imaging, improving the appreciation of lung sliding and B-lines. Should this not be available as a preset, then the settings can be adjusted manually. Further, the presence of lung sliding can be made more obvious by adjusting the focal zone to the level of the pleural line and reducing gain.

In the scanning scheme we recommend, a six-point technique on each side of the chest represents an efficient and pragmatic approach to the evaluation of the distribution and the pattern of disease[19] (Figure 10). The ultrasound transducer should be positioned perpendicular to the skin in order to image the hyperechoic pleural line and its associated lung sliding, where the visceral and parietal pleura slide over one another with respiration, and the related shimmer in the subpleural space. A-lines are reverberation artifacts arising from the repeated reflection of the ultrasound wave between the pleural line and the ultrasound transducer, and are seen as horizontal lines below the level of the pleura, with the distance between them corresponding to that between the pleura and the ultrasound transducer (Figure 11A). They indicate the presence of air, but do not differentiate between alveolar air and pleural air, and hence are present in both well aerated lungs and pneumothoraces. Unlike well aerated lungs, however, lung sliding is not present in pneumothoraces. Longitudinal orientation of the ultrasound transducer leads to the visualisation of the pleural line between the acoustic shadows of the neighbouring ribs, resulting in a bat-like image (Figure 11B), while transverse orientation of the ultrasound transducer obviates this unfavourable influence of the ribs on the generated image. Each scanning zone should be scanned for at least the duration of one respiratory cycle or 5–6 seconds.

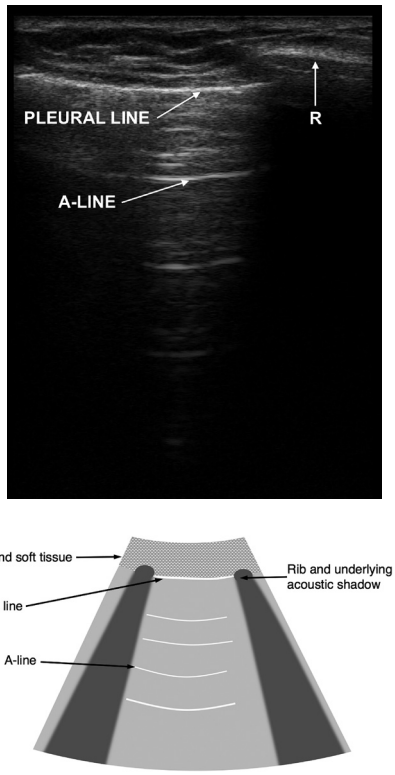

Figure 11a and b: Illustration of the normal sonographic findings on lung ultrasound with the ultrasound probe in the transverse orientation. The pleural line is identified as a hyperechoic horizontal line, superficial to which are the intercostal muscles and subcutaneous tissue and deep to which is the subpleural space. A-lines can be seen deep to the pleural line as horizontal and parallel reverberation artifacts. R: rib

Sonographic signs in COVID-19

COVID-19 pneumonia is atypical for acute respiratory distress syndrome (ARDS) and manifests with a moderate degree of deaeration and an increase in extravascular lung water[20]. Its main

sonographic findings demonstrated on LUS are illustrated in Figure 12. In the progression from the mild to the more severe forms of COVID-19 pneumonia, the ratio of air to fluid continues to decrease and incremental deaeration occurs[15].

In sonographic interstitial syndrome, where oedema is present in the interstitium, the juxtaposition of alveolar air and septal thickening causes artifacts known as B-lines to appear, reflecting the partial loss of aeration of the lung. They are displayed as discrete and vertical hyperechoic lines that arise from the pleural line and extend to the depths of the image, move synchronously with lung sliding, and replace A-lines. It is not uncommon to see one or two B-lines between the acoustic shadows of two neighbouring ribs in the lung bases of older patients, although three or more B-lines are suggestive of underlying pathology. In mild COVID-19 pneumonia, B-lines may not be found in all lung scanning zones as the disease is often multifocal (Figure 12A & 12B). Should the severity of the COVID-19 pneumonia be at least moderate, then the B-lines increase in number, become more closely spaced and eventually coalesce (Figure 12C & 12D). In sonographic alveolar syndrome, consolidation is imaged as an ill-defined and poorly echogenic focus below the pleural line with the presence of B-lines at the margins, or as hepatisation of the lung where it resembles the liver in echogenicity owing to its high fluid content. If the severity of COVID-19 pneumonia is severe, then the sonographic changes are principally found in the posterobasal region (Figure 12E). In addition to these particular sonographic signs, LUS can identify: first, the extent of extravascular lung water, indicated by the presence of B-lines which, in combination with echocardiographic assessment of the left ventricular function and doppler evaluation of the inferior vena cava, hepatic vein, portal vein, and/or renal vein for venous congestion, may help guide fluid management strategies; second, despite being uncommon in COVID-19 pneumonia, anechoic pleural effusions are often found in critically ill patients and, if present, other diagnoses should be considered; and third, the presence of pneumothorax as a complication of mechanical ventilation.

COVID-19 pneumonia is heterogenous in its presentation, but commonly there is a gradual transition from the initial predominance of a multifocal ground-glass appearance to a more dense and diffuse consolidation as the disease progresses[21]. Two phenotypes have been recognised at the severe end of the clinical spectrum[20]. In the L type, the predominant phenotype, hypoxia is common and lung compliance is normal. On LUS, B-lines can be seen. In the H type, which resembles ARDS, lung recruitment with prone positioning and increased positive end-expiratory pressure is beneficial. On LUS, consolidation is visualised. Of importance, the management strategies applicable to the L type of COVID-19 pneumonia are not effective for the H type and can indeed lead to harm[20].

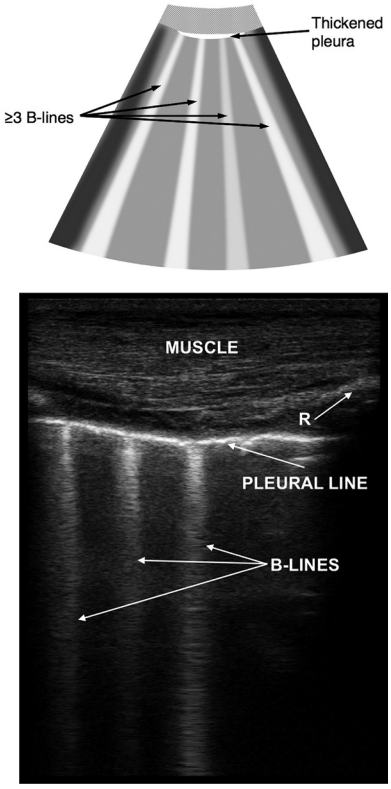

Figure 12a and b: In mild COVID-19 pneumonia, with the ultrasound probe in the transverse orientation, the pleural line is irregular and thickened. More than two B-lines are present between the ribs, and are seen as hyperechoic, non-fading and vertical comet tail-like lines extending from the pleural line to the bottom of the screen. They move in synchronisation with respiration and obliterate A-lines. R: rib

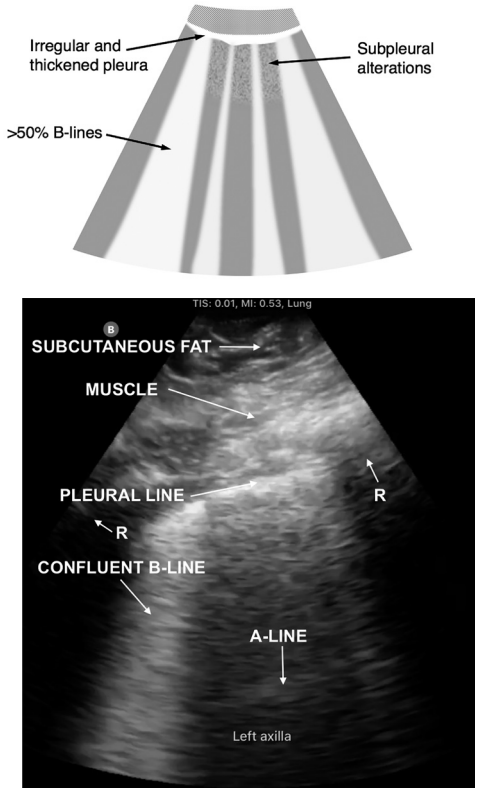

Figure 12c and d: In moderate COVID-19 pneumonia, with the ultrasound probe in the transverse orientation, multiple irregular and thickened pleural lines are seen, reflecting subpleural thickening. The subpleural alterations represent consolidation. B-lines are confluent and diffuse, resulting in a curtain-like pattern covering more than 50% of the width of the screen. R: rib

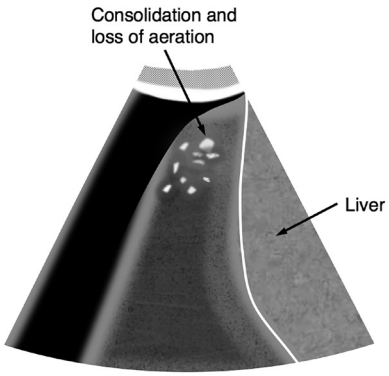

Figure 12e: In severe COVID-19 pneumonia, with the ultrasound probe in the transverse orientation, deaeration is more marked with compressed and consolidated lung, changes which are more prominent in the posterobasal zone. Lung tissue hepatisation can be seen, where the macroscopic pathological alteration of lung tissue is such that it resembles liver tissue

The utility of lung ultrasound for COVID-19

Like other modalities for the investigation of COVID-19 pneumonia, our knowledge and understanding in respect to the use of LUS continues to evolve[4]. Its fundamental applications to this new disease include its risk stratification, early evaluation of the severity, monitoring of the progression of COVID-19 pneumonia, and the identification of concomitant pathology that might influence management. LUS is hence a valuable technique for enabling clinical decision making and informing the selection of the appropriate treatment strategy. It is not, however, diagnostic of COVID-19 itself[18], although pleural line and subpleural abnormalities have been associated with a high probability of its presence relative to other causes[16]. Recently, Volpicelli et al. quantified the diagnostic accuracy of LUS against the reference standard of reverse transcription polymerase chain reaction (RT-PCR). LUS studies on the included patients were classified as either intermediate probability, for example with unilateral B-lines, or high probability, for instance with bilateral confluent B-lines and subpleural consolidations. If either intermediate or high probability findings on LUS were incorporated to rule in COVID-19, sensitivity was 90% but specificity was only 53%. If solely high probability findings on LUS were used, sensitivity decreased to 60% but specificity increased to 89%. Such results suggest that there is in fact a spectrum of sonographic signs in COVID-19, and that the selected threshold for diagnosis can have a significant impact on test characteristics[22].

The strengths of LUS in the context of COVID-19 pneumonia are its portable and point-of-care nature, facilitating rapid and safe examination with immediate results and without the need to transfer the patient outside of the clinical care environment to the radiology suite. LUS is a sensitive investigation for the early detection of pleural and interstitial pathology and has a high negative predictive value[23]. Crucially, its findings correlate well with computed tomography and, in fact, pleural line thickening and B-lines on ultrasound correspond to the ground glass appearances seen on the latter[24]. Moreover, the findings from LUS findings correlate with histopathological findings, B-lines and subpleural consolidation correspond to diffuse alveolar lung damage, while pleural line thickening and dense consolidation correlate with more severe fibroproliferative disease[25].

The limitations and pitfalls of LUS, however, should be taken into consideration. First, the diagnostic accuracy and the interpretation of the nuances of LUS are dependent upon sufficient experience and training of the ultrasonographer. Second, the distribution of the lung disease secondary to COVID-19 is non-homogenous and topographical, accentuating the need to scan all six zones of the chest, reducing the risk of failing to diagnose pathology which is patchy in nature. Third, it may be difficult to obtain ultrasound images of the posterolateral aspects of the lungs in supine and critically ill patients, particularly those of whom are mechanically ventilated. Fourth, conditions such as obesity and subcutaneous emphysema and dressings applied to the chest interfere with the transmission of ultrasound. Last, in view of the potential for interaction between the lungs and the heart, it is important to perform cardiac and diaphragmatic ultrasound in order to complete a comprehensive review with ultrasound.

CONCLUSION

In conclusion, in order to optimise ultrasound imaging and interpret ultrasound related artifacts, an understanding of the physics of ultrasound is valuable. The operator has the ability to control the appearance and the quality of the image on the monitor of the ultrasound machine by changing the characteristics of the ultrasound wave that is being emitted and manipulating how the returning ultrasound wave is processed. Further, ultrasound for lung scanning is starting to reveal its utility as a valuable point-of-care investigation in evaluating the progression of COVID-19 pneumonia and providing a radiological adjunct similar to computed tomography in clinical decision making.

REFERENCES AND FURTHER READING

1. Chan V, Perlas A. Basics of Ultrasound Imaging. In: Narouze S, editor. Atlas of Ultrasound-Guided Procedures in Interventional Pain Management. Springer New York LLC; 2011. p. 13–9.
2. Sippel S, Muruganandan K, Levine A, Shah S. Use of ultrasound in the developing world. *Int J Emerg Med*. 2011; **4(1)**: 72.
3. Roche D, Iohom G. Point-of-care ultrasound in anaesthesia and intensive care medicine. Vol. 25, *Romanian Journal of Anaesthesia and Intensive Care*. 2018. p. 95–6.
4. Smith MJ, Hayward SA, Innes SM, Miller A. Point-of-care lung ultrasound in patients with COVID-19 – a narrative review. *Anaesthesia*. 2020;
5. Havelock T, Teoh R, Laws D, Gleeson F. Pleural procedures and thoracic ultrasound: British Thoracic Society pleural disease guideline 2010. *Thorax*. 2010 Aug 1; **65(SUPPL. 2)**: i61–76.
6. Bodenham A, Babu S, Bennett J, Binks R, Fee P, Fox B, et al. Association of Anaesthetists of Great Britain and Ireland: Safe vascular access 2016. *Anaesthesia*. 2016 May 1; **71(5)**: 573–85.
7. Henderson M, Dolan J. Challenges, solutions, and advances in ultrasound guided regional anaesthesia. *BJA Educ*. 2016; **16(11)**: 374–80.
8. Carty S, Nicholls B. Ultrasound-guided regional anaesthesia. Contin Educ Anaesthesia, *Crit Care Pain*. 2007; **7(1)**: 20–4.
9. Bakhru RN, Schweickert WD. I. Physics, equipment, and image quality. *Ann Am Thorac Soc*. 2013; **10(5)**: 540–8.
10. Bushberg J, Seibert JA, Leidholdt E, Boone J. Ultrasound. In: The Essential Physics of Medical Imaging. Lippincott Williams & Wilkins; 2011. p. 500–76.

11. Ng A, Swanevelder J. Resolution in ultrasound imaging. Contin Educ Anaesthesia, *Crit Care Pain*. 2011; **11(5)**:186–92.
12. Brull R, Macfarlane AJR, Tse CCH. Practical knobology for ultrasound-guided regional anesthesia. *Reg Anesth Pain Med*. 2010; **35(2 Suppl)**: 68–73.
13. Sites B, Brull R, Chan V, Spence B, Gallagher J, Beach M, et al. Artifacts and Pitfall Errors Associated With Ultrasound-Guided Regional Anesthesia. Part II: A Pictorial Approach to Understanding and Avoidance. *Reg Anesth Pain Med*. 2007 Sep; **32(5)**: 419–33.
14. Miller A. Practical approach to lung ultrasound. *BJA Educ*. 2016; **16(2**): 39–45.
15. Peng QY, Wang XT, Zhang LN. Findings of lung ultrasonography of novel corona virus pneumonia during the 2019–2020 epidemic. *Intensive Care Med*. 2020; **46(5)**: 849–50.
16. Volpicelli G, Lamorte A, Villén T. What's new in lung ultrasound during the COVID-19 pandemic. *Intensive Care Med*. 2020; **46(7):**1445–8.
17. Volpicelli G, Elbarbary M, Blaivas M, Lichtenstein DA, Mathis G, Kirkpatrick AW, et al. International evidence-based recommendations for point-of-care lung ultrasound. *Intensive Care Med*. 2012; **38(4)**: 577–91.
18. Moore S, Gardiner E. Point of care and intensive care lung ultrasound: A reference guide for practitioners during COVID-19. Radiography [Internet]. 2020;(xxxx). Available from: https://doi.org/10.1016/j.radi.2020.04.005.
19. Lichtenstein DA, Mezière GA. Relevance of lung ultrasound in the diagnosis of acute respiratory failure the BLUE protocol. *Chest*. 2008; **134(1)**: 117–25.
20. Gattinoni L, Chiumello D, Caironi P, Busana M, Romitti F, Brazzi L, et al. COVID-19 pneumonia: different respiratory treatments for different phenotypes? *Intensive Care Med*. 2020; **46(6)**: 1099–102.
21. Shi H, Han X, Jiang N, Cao Y, Alwalid O, Gu J, et al. Radiological findings from 81 patients with COVID-19 pneumonia in Wuhan, China: a descriptive study. *Lancet Infect Dis*. 2020; **20(4)**: 425–34.
22. Volpicelli G, Gargani L, Perlini S, Spinelli S, Barbieri G, Lanotte A, et al. Lung ultrasound for the early diagnosis of COVID-19 pneumonia: an international multicenter study. *Intensive Care Med*. 2021; **47(4)**: 444–54.
23. Chiumello D, Umbrello M, Sferrazza Papa GF, Angileri A, Gurgitano M, Formenti P, et al. Global and Regional Diagnostic Accuracy of Lung Ultrasound Compared to CT in Patients With Acute Respiratory Distress Syndrome. *Crit Care Med*. 2019; **47(11)**: 1599–606.
24. Lichtenstein D, Goldstein I, Mourgeon E, Cluzel P, Grenier P, Rouby JJ. Comparative Diagnostic Performances of Auscultation, Chest Radiography, and Lung Ultrasonography in Acute Respiratory Distress Syndrome. *Anesthesiology*. 2004; **100(1)**: 9–15.
25. Almeida Monteiro RA, de Oliveira EP, Nascimento Saldiva PH, Dolhnikoff M, Duarte-Neto AN, da Silva LFF, et al. Histological–ultrasonographical correlation of pulmonary involvement in severe COVID-19. *Intensive Care Med*. 2020; 2–4.